Brown carbon and internal mixing in biomass burning particles

Daniel A. Lack[a,b,1], Justin M. Langridge[a,b], Roya Bahreini[a,b], Christopher D. Cappa[c], Ann M. Middlebrook[a], and Joshua P. Schwarz[a,b]

[a]NOAA Earth System Research Laboratory, Chemical Sciences Division, 325 Broadway, Boulder, CO 80304; [b]Cooperative Institute for Research in Environmental Sciences, University of Colorado, 216 UCB, Boulder, CO 80309; and [c]Department of Civil and Environmental Engineering, University of California, Davis, CA 95616

Edited by Mark H. Thiemens, University of California San Diego, La Jolla, CA, and approved July 16, 2012 (received for review April 23, 2012)

Biomass burning (BB) contributes large amounts of black carbon (BC) and particulate organic matter (POM) to the atmosphere and contributes significantly to the earth's radiation balance. BB particles can be a complicated optical system, with scattering and absorption contributions from BC, internal mixtures of BC and POM, and wavelength-dependent absorption of POM. Large amounts of POM can also be externally mixed. We report on the unique ability of multi-wavelength photo-acoustic measurements of dry and thermal-denuded absorption to deconstruct this complicated wavelength-dependent system of absorption and mixing. Optical measurements of BB particles from the Four Mile Canyon fire near Boulder, Colorado, showed that internal mixtures of BC and POM enhanced absorption by up to 70%. The data supports the assumption that the POM was very weakly absorbing at 532 nm. Enhanced absorption at 404 nm was in excess of 200% above BC absorption and varied as POM mass changed, indicative of absorbing POM. Absorption by internal mixing of BC and POM contributed 19(±8)% to total 404-nm absorption, while BC alone contributed 54(±16)%. Approximately 83% of POM mass was externally mixed, the absorption of which contributed 27(±15)% to total particle absorption (at 404 nm). The imaginary refractive index and mass absorption efficiency (MAE) of POM at 404 nm changed throughout the sampling period and were found to be 0.007 ± 0.005 and 0.82 ± 0.43 $m^2 g^{-1}$, respectively. Our analysis shows that the MAE of POM can be biased high by up to 50% if absorption from internal mixing of POM and BC is not included.

forest fire | climate | tar balls

Particle emissions from biomass burning (BB) are a significant component of global combustion-sourced black carbon (BC) and primary particulate organic matter (POM), contributing approximately 63% and 94%, respectively (1). The radiative impact of BB emissions at regional and global scales are significant (2) and can create instantaneous top-of-atmosphere cooling or warming (up to ±10 s of Wm^{-2}), depending on surface albedo (3, 4). BB emissions from northern Eurasia and North America are often efficiently transported into the Arctic (5, 6) and contribute to climate change in that region (7), including snow and ice melt following BC deposition (8).

The radiative impacts of BB particle emissions are very different than those of particles emitted from relatively efficient (i.e., internal) fossil fuel (FF) combustion. Co-emission of strongly absorbing BC and non- or mildly absorbing POM contrast to the predominantly absorbing BC emissions of FF combustion (2, 9) and can lead to a dominance of light scattering from the POM.

The co-emission of BC and POM can additionally lead to internal mixing, which can enhance BC absorption by serving as a radiation lens. Such lensing may increase absorption by a factor of two (10–12). BC particles can be associated with significant amounts of non-BC material in the atmosphere and enhancement of ambient BC absorption is expected (13–15). Studies of direct and indirect measures of absorption enhancement confirm they can occur in the laboratory (16–19); however, there is little direct evidence from field observations. Because climate models are currently introducing enhancements to BC absorption due to the lensing effect (e.g., 20, 21), the question arises as to whether inclusion of this absorption term in models has sufficient evidence from real atmospheric systems. It seems apparent that more evidence of the occurrence and spatial and temporal distribution of the effect in the atmosphere are required.

In addition to enhanced absorption by internal mixing, POM can itself absorb radiation in the low-visible and UV wavelengths (9, 22–24) depending on the chemical functional groups (e.g., nitrated/polycyclic aromatics, phenols) within the POM (25, 26). Such POM is referred to as brown carbon (BrC). Given the large source of BB POM in the atmosphere (1), further understanding of the absorptive properties of BB POM, especially from ambient measurements, is needed.

In this work we present an attribution method for absorption and mixing state using direct measurements of multi-wavelength photo-acoustic-measured dry and thermal-denuded absorption. A glossary of terms and abbreviations is included in Table S1.

Analysis

Over a 24-h period, two BB plume events from the same fire with different optical properties were sampled. The analysis procedure, given in greater detail in *Methods*, included:

- *Confirmation of BB event*: Mass spectroscopic and optical markers of the particles confirmed that the plumes were consistent with a BB event.
- *Absorption enhancement in BB plumes*: A measure of thermal-denuded absorption at 404 and 532 nm compared to dry absorption at those wavelengths enabled determination of absorption enhancements (E_{Abs}). $E_{Abs\text{-}532}$ was found to be the same for the two events and independent of POM mass indicating that the core and coating dimensions were relatively stable and that the POM was nonabsorbing at 532 nm.
- *Absorption enhancement in BB plumes*: In contrast, $E_{Abs\text{-}404}$ was found to be dependent on POM mass due to intrinsic absorption of POM and external mixing of POM (i.e., if POM was all internally mixed $E_{Abs\text{-}532}$ would show POM mass dependence).
- *Externally mixed BB organic particles*: We assume a BC core size (constrained by measurements) and using Mie theory, optimize the coating thickness until measured and modeled $E_{Abs\text{-}532}$ match. From this the extent of external mixing was determined.

Author contributions: D.A.L. designed research; D.A.L., R.B., and J.P.S. performed research; D.A.L. and J.M.L. contributed new reagents/analytic tools; D.A.L., J.M.L., R.B., C.D.C., A.M.M., and J.P.S. analyzed data; and D.A.L., J.M.L., and C.D.C. wrote the paper.

The authors declare no conflict of interest.

This article is a PNAS Direct Submission.

Freely available online through the PNAS open access option.

[1]To whom correspondence should be addressed. E-mail: Daniel.Lack@noaa.gov.

This article contains supporting information online at www.pnas.org/lookup/suppl/doi:10.1073/pnas.1206575109/-/DCSupplemental.

- *BB brown carbon refractive index (RI)*: Using the core-coat system modeled to determine POM external mixing and an externally mixed particle size distribution (constrained by measurements), the imaginary RI of POM at 404 nm ($k_{\text{BrC-404}}$) was optimized for closure between measured and modeled $E_{\text{Abs-404}}$. The absorption at 404 nm includes terms from BC, BC internally mixed with POM, and externally mixed POM.
- *BB absorption attribution*: $k_{\text{BrC-404}}$ was used to calculate the fraction of absorption due to BC, internal mixing of BC and POM, and externally mixed POM.
- *Mass absorption efficiency (MAE) of BB organic particles*: The MAE of the POM (including enhanced absorption by internal mixing) was determined from measurements. The effect of enhanced absorption due to internal mixing was removed (using Mie theory and $k_{\text{BrC-404}}$), which made the MAE of the two events self-consistent. A significant contribution to the optical property differences of the two events was therefore internal mixing of nonabsorbing material.

Results and Discussion

Confirmation of Biomass Burning Event. A time series of mass and optical properties are shown in Fig. S1. Common chemical and optical characteristics of the particles within this plume were similar to BB plumes from other studies. Gas-phase chemical markers suggest that, for the majority of the measurement period, smoldering fire conditions were dominant (27). The relationship between the fraction of POM that is m/z 60 (f_{60}—linked to Levoglucosin from cellulose combustion) and m/z 44 (f_{44}—represents oxidized fraction of POM) provides evidence that a wide range of oxidation states of POM were sampled while in the presence of the f_{60} BB marker. The data is consistent with the analysis of BB plumes analyzed by Cubison et al. (28) (Fig. S2).

The measured absorption wavelength dependence (404–658 nm) ranged from 1.25 to 2.3 (Table 1 and Fig. S3*A*), similar to previous measurements in BB plumes (24, 29). The average single scatter albedo (SSA) of the BB particles at 404 nm was 0.85 (Table 1 and Fig. S3*B* and *SI Text*), which compares well with the SSA_{404} for Ponderosa Pine combustion particles (24) and smoldering boreal forest fires (30, 31).

Absorption Enhancement in Biomass Burning Particles. Our key observation is that, while nonrefractory particulate matter (NR-PM) mass ($m_{\text{PM-NR}}$) (and thus m_{POM}*) increased significantly within the main BB sampling periods (defined below), the $E_{\text{Abs-532}}$ varied little (1.4 ± 0.1), whereas $E_{\text{Abs-404}}$ gradually increased (from 1.7 up to 3.5) (Fig. 1 *A*–*C*). At short visible wavelengths, the observed E_{Abs} may contain absorption contributions from BC, internal mixing of BC, and other material and intrinsic absorption by POM that is either internally or externally mixed (32). The difference in response of $E_{\text{Abs-532}}$ and $E_{\text{Abs-404}}$ to changes in $m_{\text{PM-NR}}$ suggests that (*i*) the POM was very weakly, or nonabsorbing at 532 nm but absorbing at 404 nm [i.e., if lensing absorption enhancement was the only additional absorption, $E_{\text{Abs-404}}$ would follow the same profile as $E_{\text{Abs-532}}$ (32)]; (*ii*) the physical properties of the particles that can affect E_{Abs} (BC core size and coating thicknesses) were sufficiently stable as to not create significant $E_{\text{Abs-532}}$ variability; and (*iii*) that the absorbing POM at 404 nm was predominately externally mixed with BC. Given that coating thickness remained relatively constant $E_{\text{Abs-404}}$ increases are likely from increases in externally mixed absorbing POM (32).

Four time periods are defined based on the evolving $m_{\text{PM-NR}}$ and E_{Abs} (shown in Fig. 1*A* as the shaded areas and defined in Table 1 and Table S2). BG1 and BG2 represent background conditions, BB dominates period BB1 and BB2 although BB2 is likely mixed with anthropogenic pollution (morning commuter traffic). With these time period definitions, we note a second key observation. $E_{\text{Abs-404}}$, during periods BB1 and BB2, exhibited different relationships with $m_{\text{PM-NR}}$ (Fig. 1*B*); evidence that the absorption properties of the BrC evolved during the event. This evolution may be from variations in the combustion conditions of the fire, atmospheric processing, or mixing. High RH may enhance absorption [through lensing and POM functional group processing (17, 33)]; however, the average and maximum ambient RH during the sampling period was 28% and 46%, respectively, (34) and the measurement RH was &*lt*; = 25%, making it unlikely that RH contributed to the observed enhancements.

We emphasize that $E_{\text{Abs-532}}$ contains no intrinsic POM absorption term, and it is therefore a quantity linked to internal mixing of BC only, whereas $E_{\text{Abs-404}}$ is linked to both internal and external mixtures. This clarification is important for consideration of BB plumes where externally mixed POM, and thus intrinsic POM absorption, is significant (9, 35, 36).

Externally Mixed Biomass Burning Organic Particles. Most of the observed POM is likely externally mixed [results above and (37)], the extent of which can impact the observed E_{Abs} from internal mixing and POM absorption (32). Interpretation of our measurements in terms of the specific absorptive properties of POM, such as RI and MAE, requires understanding of the mixing state of the sampled aerosol.

We estimate the particle mixing state (i.e., the distribution of NR-PM between BC-containing and non-BC particles) through a combined optical/mass closure method where it is assumed that (*i*) POM and ammonium nitrate is nonabsorbing at 532 nm and (*ii*) the system can be accurately modeled using spherical particles (see *Methods*). Fig. 1*C* and other studies suggest both of these assumptions are valid (9, 24, 35). Core-shell Mie Theory is used to calculate a coating growth factor (CF) for the NR-PM coating on BC that reproduces the measured $E_{\text{Abs-532}}$ (Figs. S4 and S5). The average count median diameter from the SP2 was used to model d_{Core}. The BC core distribution accumulated an even coating of NR- PM such that

$$d_{\text{Total}} = d_{\text{Core}} \times CF. \quad [1]$$

For reference, given the BC size distribution, to obtain $E_{\text{Abs}} = 1.4$ (mean value at 532 nm) requires CF of 1.45, which corresponds to a coating thickness of 32 nm. Once the coating thickness is known, the remaining $m_{\text{PM-NR}}$ is assumed externally mixed.

We estimate that the fraction of PM (and POM*†) mass that is externally mixed ($f_{\text{PM-Ext}}, f_{\text{POM-Ext}}$) is $83(\pm 14)\%$ (Fig. 2*A*), which is an upper limit as the thermal denuder is unlikely to remove all POM from BC cores. Our result compares favorably to that of Kondo et al. (37), who measured an $f_{\text{POM-Ext}}$ of 83% for several North American BB plumes. Semi-quantitative estimates of the number fraction of non-BC-containing particles were determined from the SP2. During BB1 and BB2, approximatley 85% of all particles detected by the SP2 did not contain detectable BC, while during BG1 and BG2, only 65% of the particles appeared BC-free. Note that the SP2 was not configured to produce quantitative estimates of mass of externally mixed material (see *SI Text*).

Biomass Burning Brown Carbon Refractive Index. Using the observed wavelength-dependent E_{Abs} and our estimate of the BC/POM mixing state, a time series of the imaginary RI of the POM (i.e. "brown carbon") at 404 nm can be determined.

We apply Mie Theory at 404 nm to the BC core, the BC core/NR-PM coat distribution, and the remaining externally mixed POM and find the imaginary RI for POM ($k_{\text{BrC-404}}$) that matches the measured $E_{\text{Abs-404}}$ (see *Methods* and Fig. S6). The average count median (volume equivalent) diameter of PM from the AMS was used to model the externally mixed POM.

*Ammonium nitrate is non-absorbing (at 532 and 404 nm) (56).

†See uncertainties and assumptions section.

Table 1. Average measured and derived particle optical and physical characteristics across the sampling periods

	Measured					Derived				
PeriodLabel-Details	SSA 404 nm	SSA 532 nm	AAE 658–404 nm	$E_{Abs-404}$	$E_{Abs-532}$	MAE_{BC} 404/532	MAE_{PM} 404/532	$f_{POM-Ext}$	k_{BrC} 404 nm	MAE_{BrC} 404 nm $m^2 g^{-1}$
BG1: Background/Low Signal	0.83	0.80	1.4	1.5	1.3	5.8/5.8	8.4/7.0	0.80	0.004	0.6
BB1: BB	0.85	0.90	2.3	2.5	1.4	5.3/5.6	12.9/8.3	0.89	0.009	1.0
BB2: BB+Anthropogenic	0.80	0.84	2.3	2.1	1.5	6.4/5.6	13.8/8.1	0.79	0.005	1.1
BG2: Background/Low Signal	0.83	0.75	1.1	1.3	1.3	6.2/6.4	7.9/7.3	0.79	0.006	0.2

The average $k_{BrC-404}$ was 0.007(±0.005), with the largest $k_{BrC-404}$ of 0.015 found during period BB1. The calculated $k_{BrC-404}$ suggests that there is a large variability in the optical properties of the POM (factors of 2–3) even within the same BB event (Fig. 2*B*). The average $k_{BrC-404}$ for period BB1 was found to be 0.009, which is at the lower end reported in previous studies (16, 38, 39). Interestingly, BB2, which shows significant absolute BrC absorption, has a $k_{BrC-404}$ of around 0.005, indicating that the BrC is chemically different than that in BB1, or it has mixed with nonabsorbing material from other sources (such as anthropogenic POM).

Biomass Burning Absorption Attribution. Having established that BC, internal mixing, and absorbing POM are all contributors to the total absorption at 404 nm, we now quantitatively partition these effects. We use the calculated CF, $k_{BrC-404}$ and some additional Mie Theory modeling to calculate the fraction of total absorption due to uncoated BC (f_{Abs-BC}), internal mixing ($f_{Abs-Lens}$), and BrC ($f_{Abs-BrC}$) (*Methods* and Fig. S7).

We find that BC absorption does not always dominate the total absorption within the BB plume. The BC contributed 54(±16)% of total 404 nm absorption while internal mixing contributed 19(±8)% (shown in Fig. 3*B* as histograms). Even though the POM is calculated to have a $k_{BrC-404}$ value significantly lower than BC ($k_{BrC-404} = 0.01$, $k_{BC} = 0.71$), BrC absorption from internally and externally mixed POM contributed 27(±15)% of total 404 nm absorption (Fig. 3 *A* and *B*). Despite the modest absorption properties of BrC, the large POM mass in the BB plumes (20–50 times greater than BC mass) produced significant absorption at 404 nm.

The fractional absorption histograms for BC and lensing absorption enhancement at 532 nm are also included in Fig. 3*B*.

Mass Absorption Efficiency of Biomass Burning Organic Particles. The MAE is an alternative quantitative measure of the absorptive properties of POM. MAE_{BrC} at 404 nm can be calculated from the partitioned absorption and measured POM mass. Calculations of a *bulk* MAE_{BrC} are highly variable, ranging between 1–2.5 $m^2 g^{-1}$ (Fig. 4*A*). The bulk MAE_{BrC} includes absorption from lensing enhancement and is an overestimate of the true MAE of the POM. Excluding the internal mixing contribution (Fig. 3) produces actual MAE_{BrC} values of 0.5–1.5 $m^2 g^{-1}$ (Fig. 4*A*) indicating that internal mixing can lead to MAE_{BrC} overestimates of 50% or more. Periods BB1 and BB2 have very different bulk MAE_{BrC} (Fig. 4*B*); however, when the contribution of internal mixing is removed (i.e., actual MAE_{BrC}; Fig. 4*C*) the MAE_{BrC} of the previously different periods converge, indicating that the additional POM in period BB2 was non-absorbing at 404 nm and created additional absorption through internal mixing with BC.

Summary. In this paper we analyzed optical measurements of particles from a large Ponderosa Pine forest fire to assess the contribution of radiation absorption by BC, absorption through internal mixing of BC with POM and ammonium nitrate (lensing effect), and intrinsic absorption of POM (brown carbon).

We present evidence of lensing-driven enhanced absorption at 532 nm, up to 1.7 times (mean = 1.38), due to internal mixing of biomass combustion sourced BC with POM and ammonium nitrate.

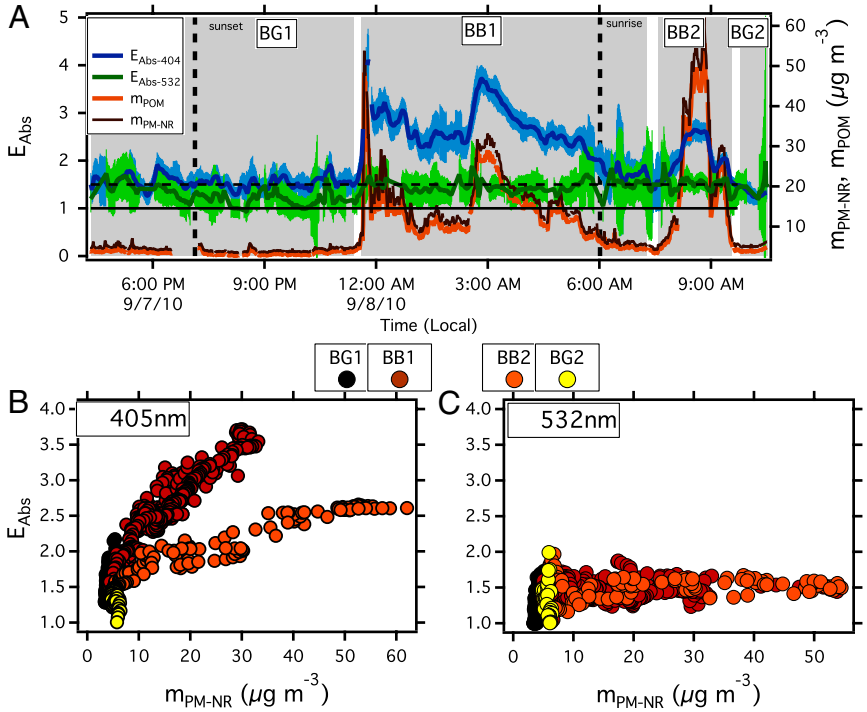

Fig. 1. Measured absorption enhancements (E_{Abs}). (*A*) Time series of $E_{Abs-404}$ and $E_{Abs-532}$ and NR-PM and POM mass. One-second optical data overlaid on the 60-second data. Horizontal solid and dashed line indicate an E_{Abs} of 1.0 and 1.5, respectively. Sunrise and sun set = vertical dashed lines. (*B* and *C*) $E_{Abs-404}$ and $E_{Abs-532}$ respectively versus NR-PM mass colored by time periods identified in the shaded regions of *A* and identified in Table 1 and Table S2.

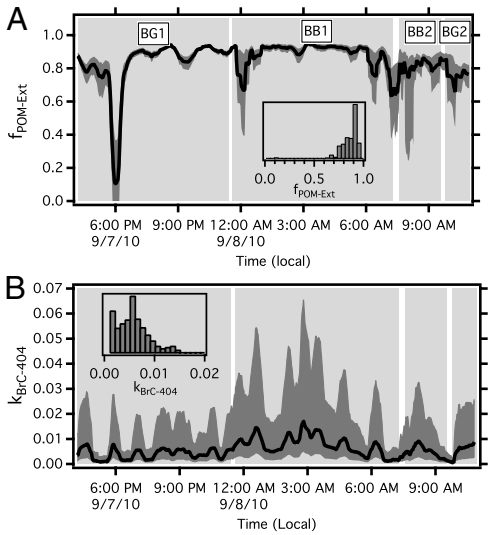

Fig. 2. (*A*) Calculated fraction of POM that is externally mixed ($f_{POM-Ext}$). (*B*) Calculated imaginary refractive index of POM ($k_{BrC-404}$). Shaded area indicates propagated uncertainties. Histograms of each parameter shown as inset to each graph.

For the BB particles studied, lensing absorption enhancement can only occur within internal mixtures of BC and POM (or ammonium nitrate), and so it is significant that we find that 83% of NR-PM (and POM) within this plume is externally mixed from BC. Previous studies recognize this effect (9, 35, 37); however, our data serves to highlight the importance of this effect on the optics of the internal and external mixed particles.

The measured POM was very weakly absorbing or nonabsorbing at 532 nm and showed strong variability in absorption strength at 404 nm. A time series of the imaginary refractive index for POM ($k_{BrC-404}$) was calculated and indicated large variability (factors of 2–3) even within the same BB event. Three absorption sources contributed to total absorption in the BB plume at 404 nm. The internal mixing component contributed 19(±8)% of total 404 nm absorption, while both internally and externally mixed POM contributed 27(±15)% even though the POM has a k_{BrC} value significantly lower than BC (0.01 compared to 0.71). This is because the POM mass is a factor of 20–50 times greater

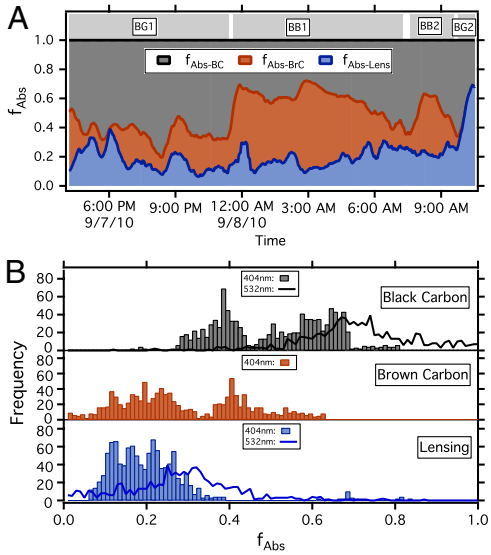

Fig. 3. Particle absorption sources within the biomass burning plume. (*A*) Fraction of absorption at 404 nm by BC (f_{Abs-BC}), BrC ($f_{Abs-BrC}$), and internal mixing ($f_{Abs-Lens}$). (*B*) Histograms of fractional absorption at 404 nm for BC, BrC and internal mixing at 404 nm. Histograms for 532 nm included as solid lines.

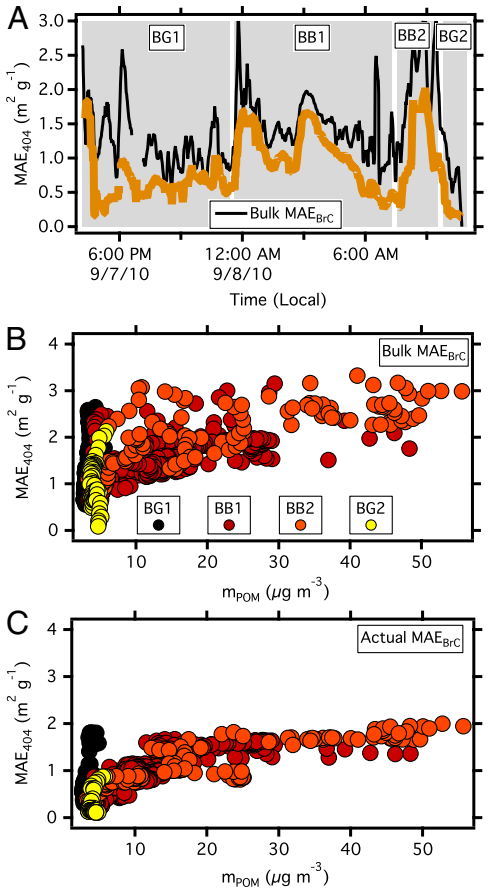

Fig. 4. Calculated mass absorption efficiencies of brown carbon at 404 nm. (*A*) Time series of bulk (black) and actual MAE_{BrC} (brown). (*B*) Bulk and (*C*) actual MAE_{BrC} vs m_{POM} colored by the periods defined in Table 1 and Table S1.

than the BC mass. As with $k_{BrC-404}$, the calculated MAE_{BrC} were highly variable across the BB event due in part to mixing of the absorbing with nonabsorbing POM and increased enhancement effect for at least one period BrC absorption from internally of sampling. Variability may also come from differences in combustion phases of the fire.

This dataset is among the only pieces of direct evidence showing the importance of absorption by internal mixing and externally mixed brown carbon in BB plumes. The unique photo-acoustic measurements of dry and thermal-denuded absorption at multiple wavelengths reveal the complicated picture of BB particle optics and shows the dimensions to particle absorption that is not captured by common absorption measurement methods.

Methods

Experimental. The Four-Mile Canyon forest fire started burning on September 6. 2010, approximately 15 km from the NOAA ESRL laboratories in Boulder, Colorado. It burned 6,200 acres of Ponderosa Pine forest and 168 houses over 11 d (40). Twenty-four hours after ignition of the fire, gas and particle sampling of the fire plume commenced through rooftop sampling ports of the NOAA laboratory. Dry particle extinction (662, 532, and 405 nm) were measured using a cavity ring down spectrometer (CRDS, ref. 41). A photo-acoustic aerosol absorption spectrometer (PAS) measured total absorption at 658, 532, and 404 nm ($b_{Abs-658}$, $b_{Abs-532}$, $b_{Abs-404}$) and thermal-denuded absorption (sample heated to 200 °C) at 532 and 404 nm ($b_{Abs-532-BC}$, $b_{Abs-404-BC}$) (42). From these measurements the following absorption-related properties were calculated: (*i*) absorption enhancements at 532 and 404 nm ($E_{Abs-532}$, $E_{Abs-404}$) using Eqs. **2** and **3**; (*ii*) absorption angstrom exponent (AAE) using Eq. **4**; and (*iii*) single scatter albedo (SSA) using Eq. **5**:

$$E_{\text{Abs-532}} = \frac{b_{\text{Abs-532}}}{b_{\text{Abs-532-BC}}} = \frac{b_{\text{Abs-532-BC}} + b_{\text{Abs-532-Lens}}}{b_{\text{Abs-532-BC}}}, \quad [2]$$

EARTH, ATMOSPHERIC, AND PLANETARY SCIENCES

$$E_{\text{Abs-404}} = \frac{b_{\text{Abs-404}}}{b_{\text{Abs-404-BC}}} = \frac{b_{\text{Abs-404-BC}} + b_{\text{Abs-404-Lens}} + b_{\text{Abs-404-BrC}}}{b_{\text{Abs-404-BC}}}, \quad [3]$$

$$\text{AAE} = \frac{\ln\left(\frac{b_{\text{Abs}}(\lambda_1)}{b_{\text{Abs}}(\lambda_2)}\right)}{\ln\left(\frac{\lambda_1}{\lambda_2}\right)}, \quad [4]$$

$$\text{SSA} = \frac{b_{\text{Ext}} - b_{\text{Abs}}}{b_{\text{Ext}}}. \quad [5]$$

E_{Abs} values reported here are a lower limit as the thermal denuder, which heats the aerosol to 200 °C, is unlikely to remove all of the non-BC material (43). The PAS technique has been validated for accurate measurement of E_{Abs} (18) and does not show biases to POM that may occur on filter-based absorption methods (44). Total nonrefractory particle mass ($m_{\text{PM-NR}}$) and mass size distributions were measured using an compact time-of-flight aerosol mass spectrometer (AMS, ref. 45). $m_{\text{PM-NR}}$ consisted of POM (90%) and ammonium nitrate (10%) (Fig. 1*A* and Fig. S8). An analysis of the mass to charge (m/z) ratios of 30 and 46 showed that the nitrate was associated with ammonium rather than POM (46) (see *SI Text*). Black carbon mass and microphysical state were measured using a single particle soot photometer (SP2) (15). Sample flow was dried to &*lt*; = 25% RH prior to measurement. Ambient RH was, on average only 28% (34). All data were averaged from the nominal collection rate of each instrument to 1 minute. Time series of extinction, absorption, and NR-PM, POM, and BC mass are shown in Fig. S1. For the signal levels measured and time resolution reported, measurement uncertainties are estimated as follows: AMS-±38, SP2-±40%, PAS 532 and 658 nm-±5%, PAS 404 nm-±10%, CRD dry-±1%. Further details on PAS and SP2 calibration and AMS mass balance are provided in *SI Text*.

Modeling. The core-shell application of Mie Theory (47) was used for further interpretation of the data.† An average log-normal fit to all SP2-measured BC size distributions and all AMS-measured POM and ammonium nitrate size distributions were used to model the BC core and externally mixed material respectively.† The average BC count median diameter from the SP2 was found to be 140 ± 10 nm (with a log-normal standard deviation of 1.3), which is within reported ranges for BB BC (37, 48). The count equivalent diameter of the NR-PM was measured by the AMS and the average found to be 190 ± 30 nm (with a log-normal standard deviation of 1.7), which is consistent with previous studies of BB particles (49). Further details are provided in *SI Text*.

Calculation of Externally Mixed Biomass Burning Organic Particles. For each data point in the time series we

1. apply a CF to the BC core distribution and calculate the absorption cross-section (σ_{Abs}) using assumed RIs†;
2. calculate $E_{\text{Abs-532-Mod}}$ from σ_{Abs} of the core and coated distributions;
3. optimized CF until the Mie Theory-calculated $E_{\text{Abs-532-Mod}}$ matches $E_{\text{Abs-532}}$;
4. calculate the volume fraction of core and coating material by applying the optimized CF to the core distribution;
5. calculate the mass fraction of BC (f_{BC}) and the POM/ammonium nitrate ($f_{\text{PM-NR}}$) using assumed densities of BC and for POM/ammonium nitrate†;
6. calculate the mass of coating (internally mixed NR-PM, $m_{\text{PM-NR-Int}}$) by anchoring f_{BC} to BC mass (m_{BC} from SP2)

$$m_{\text{PM-NR-Int}} = \frac{m_{\text{BC}}}{f_{\text{BC}}} \times f_{\text{PM-NR}}; \quad [6]$$

7. calculate the mass fraction of externally mixed NR-PM ($f_{\text{PM-NR-Ext}}$) by comparison of $m_{\text{PM-NR-Int}}$ to $m_{\text{PM-NR}}$ measured by the AMS

$$f_{\text{PM-NR-Ext}} = 1 - \frac{m_{\text{PM-NR-Int}}}{m_{\text{PM-NR}}}; \quad [7]$$

8. assume that the extent of external mixing of PM is the same as that of POM†:

$$f_{\text{PM-NR-Ext}} = f_{\text{POM-Ext}}. \quad [8]$$

Calculation of Biomass Burning Brown Carbon Refractive Index.

1. 404 nm σ_{Abs} of the BC core ($\sigma_{\text{Abs-404-BC}}$) is calculated using assumed RIs†;
2. 404 nm σ_{Abs} of the BC core coated in absorbing POM (initial guess at $k_{\text{BrC-404}}$) according to the optimized CF ($\sigma_{\text{Abs-404-BC-Lens-BrC}}$) is calculated;
3. σ_{Abs} of the externally mixed POM is calculated using the average AMS size distribution ($\sigma_{\text{Abs-404-BrC-Ext}}$) †.
4. $\sigma_{\text{Abs-404-BrC-Ext}}$ is scaled by $\frac{1}{1-f_{\text{POM-Ext}}}$; which ensures the absorption for the complete system (internally mixed BC-POM and externally mixed POM) has a contribution from one internally mixed particle and $\frac{1}{1-f_{\text{POM-Ext}}}$ externally mixed particles. Here we assume that absorption scales linearly with volume (50).†
5. $E_{\text{Abs-404-Mod}}$ calculated:

$$E_{\text{Abs-404-Mod}} = \frac{\sigma_{\text{Abs-404-BC-Lens-BrC}} + \sigma_{\text{Abs-404-BrC-Ext-Scaled}}}{\sigma_{\text{Abs-404-BC}}}, \quad [9]$$

6. $k_{\text{BrC-404}}$ optimized until $E_{\text{Abs-404-mod}} = E_{\text{Abs-404}}$.

Calculation of Biomass Burning Absorption Attribution and Mass Absorption Efficiency of Biomass Burning Organic Particles. (Note: Parameters with an asterisk denote measured data.)

1. Mie Theory is used to calculate two versions of absorption enhancement:

$$E_{\text{Abs-404-All-Mod}} = \frac{\sigma_{\text{Abs-404-BC-Lens-BrC}}}{\sigma_{\text{Abs-404-BC}}}, \quad [10]$$

$$E_{\text{Abs-404-NoBrC-Mod}} = \frac{\sigma_{\text{Abs-404-BC-Lens-BrC}} - \sigma_{\text{Abs-404-BrC-Int}}}{\sigma_{\text{Abs-404-BC}}}, \quad [11]$$

$\sigma_{\text{Abs-404-BC}}$: σ_{Abs} due to a BC core of diameter d_{Core}.
$\sigma_{\text{Abs-404-BC-Lens-BrC}}$: σ_{Abs} of the BC core coated in absorbing POM with particle diameter of $d_{\text{Total}}(\text{CF} \times d_{\text{Core}})$. Includes absorption from BC core, lensing effect of coatings on BC and intrinsic absorption of coating. Calculated imaginary refractive index for POM ($k_{\text{BrC-404}}$) is used.
$\sigma_{\text{Abs-404-BrC-INT}}$: As for $\sigma_{\text{Abs-404-BC-Lens-BrC}}$ but with a nonabsorbing core having the same real RI for the core and coat. This determines the intrinsic absorption cross section of just the absorbing POM coating. Effects of lensing are removed.

2. Non-BC absorption of the coated particles is calculated:

$$b_{\text{Abs-404-Lens-BrCInt}} = (E_{\text{Abs-404-All-Mod}} - 1) \times {*b}_{\text{Abs-404-BC}}. \quad [12]$$

3. Lensing absorption enhancement of the coated particles is calculated:

$$b_{\text{Abs-404-Lens}} = (E_{\text{Abs-404-NoBrC-Mod}} - 1) \times {*b}_{\text{Abs-404-BC}}. \quad [13]$$

4. Fraction of 404-nm absorption due to BC, non-BC absorption, additional BC absorption due to lensing, and BrC is calculated ($f_{\text{Abs-BC}}$, $f_{\text{Abs-NonBC}}$, $f_{\text{Abs-Lens}}$ and $f_{\text{Abs-BrC}}$):

$$f_{\text{Abs-BC}} = \frac{{*b}_{\text{Abs-404-BC}}}{{*b}_{\text{Abs-404}}}, \quad [14]$$

$$f_{\text{Abs-NonBC}} = 1 - f_{\text{Abs-BC}}, \quad [15]$$

$$f_{\text{Abs-Lens}} = \frac{b_{\text{Abs-404-Lens}}}{{*b}_{\text{Abs-404}}}, \quad [16]$$

$$f_{\text{Abs-BrC}} = 1 - f_{\text{Abs-BC}} - f_{\text{Abs-Lens}}. \quad [17]$$

5. MAE for POM including BrC and lensing absorption enhancement ($\text{MAE}_{\text{BrC-Lens}}$), and for POM including just BrC absorption (MAE_{BrC}) is calculated.

$$\text{MAE}_{\text{BrC-Lens}} = \frac{{*b}_{\text{Abs-404}} - {*b}_{\text{Abs-404-BC}}}{{*m}_{\text{POM}}}, \quad [18]$$

$$\text{MAE}_{\text{BrC}} = \frac{{*b}_{\text{Abs-404}} - ({*b}_{\text{Abs-404-BC}} + b_{\text{Abs-404-Lens}})}{{*m}_{\text{POM}}}. \quad [19]$$

Uncertainties and Assumptions. Throughout the analysis of the data presented, certain assumptions have been made, and, where possible, uncertainties assigned to these assumptions. These uncertainties were then used to determine the uncertainty range in the parameters derived through the modeling procedures using a Monte Carlo simulation (100 simulations).

We assume:

1. Mie Theory can be used to model this system (i.e., spherical particles) (9, 24, 35);

2. absorption scales linearly with volume (50);
3. the data for the total AMS-measured mass shows it is composed of POM and ammonium nitrate mass. We assume that both POM and ammonium nitrate are involved in coating of BC and the extent of external mixing of both species is the same. The tight correlation between POM and total PM mass (Fig. S8) indicates that POM and ammonium nitrate vary consistently.
4. Particle size distributions can be represented by a log-normal function (51) and the variability in the log-normal fits to the BC and NR-PM size distributions across the sampling period is captured by uncertainties of $\pm$10 nm for BC and $\pm$30 nm for NR-PM.
5. Densities and refractive indices (and uncertainties) for BC and NR-PM were chosen from assessment of various studies (16, 52, 53).
   a. BC density was assumed to be $1.8(\pm 0.1)$ g cm^{-3} (52);
   b. POM/Ammonium nitrate density was assumed to be $1.4(\pm 0.1)$ g cm^{-3} (54).
   c. Complex refractive indices (RI) for BC of $1.85 + 0.71i$ (52) and NR-PM of $1.5 + 0.0i$ (55)
   d. A RI uncertainty of $\pm$0.1 for BC and the real RI for NR-PM.

ACKNOWLEDGMENTS. Thanks to Charles Brock and Daniel Murphy (NOAA) for useful discussions. Funded by the National Oceanic and Atmospheric Administration Climate Program. C.D.C. acknowledges additional financial support from the National Center for Environmental Research, US Environmental Protection Agency (RD834558).

1. Bond TC, et al. (2004) A technology-based global inventory of black and organic carbon emissions from combustion. *J Geophys Res* 109:D14203.
2. Ramanathan V, Carmichael G (2008) Global and regional climate changes due to black carbon. *Nat Geosci* 1:221–227.
3. Christopher SA, Zhang J (2002) Daytime variation of shortwave direct radiative forcing of biomass burning aerosols from GOES-8 imager. *J Atmos Sci* 59:681–691.
4. Keil A, Haywood JM (2003) Solar radiative forcing by biomass burning aerosol particles during SAFARI 2000: A case study based on measured aerosol and cloud properties. *J Geophys Res* 108:8467–8476.
5. Stohl A, et al. (2007) Arctic smoke—Record high air pollution levels in the European Arctic due to agricultural fires in Eastern Europe in spring 2006. *Atmos Chem Phys* 7:511–534.
6. Warneke C, et al. (2010) An important contribution to springtime Arctic aerosol from biomass burning in Russia. *Geophys Res Lett* 37:L01801.
7. Shindell D, Faluvegi G (2009) Climate response to regional radiative forcing during the twentieth century. *Nat Geosci* 2:294–300.
8. Flanner MG, Zender CS, Randerson JT, Rasch PJ (2007) Present-day climate forcing and response from black carbon in snow. *J Geophys Res* 112:D11202, 10.1029/2006JD008003.
9. Chakrabarty RK, et al. (2010) Brown carbon in tar balls from smoldering biomass combustion. *Atmos Chem Phys* 10:6363–6370.
10. Bond T, Habib G, Bergstrom RW (2006) Limitations in the enhancement of visible light absorption due to mixing state. *J Geophys Res* 111:D20211.
11. Jacobson MZ (2001) Strong radiative heating due to the mixing state of black carbon in atmospheric aerosols. *Nature* 409:695–697.
12. Schnaiter M, et al. (2005) Absorption amplification of black carbon internally mixed with secondary organic aerosol. *J Geophys Res* 110:D19204, 10.1029/2005JD006046.
13. McMeeking GR, et al. (2011) Black carbon aerosol mixing state, organic aerosols and aerosol optical properties over the United Kingdom. *Atmos Chem Phys* 11:9037–9052.
14. Moteki N, et al. (2007) Evolution of mixing state of black carbon particles: Aircraft measurements over the western Pacific in March 2004. *Geophys Res Lett* 34:L11803.
15. Schwarz JP, et al. (2008) Measurement of the mixing state, mass, and optical size of individual black carbon particles in urban and biomass burning emissions. *Geophys Res Lett* 35:L13810.
16. Adler G, Abo Riziq A, Erlick C, Rudich Y (2009) Effect of intrinsic organic carbon on the optical properties of fresh diesel soot. *Proc Natl Acad Sci USA* 107:6699–6704.
17. Brem BT, Mena Gonzalez FC, Meyers SR, Bond TC, Rood MJ (2011) Laboratory-measured optical properties of inorganic and organic aerosols at relative humidities up to 95%. *Aerosol Sci Technol* 46:178–190.
18. Lack DA, et al. (2009) Absorption enhancement of coated absorbing aerosols: Validation of the photo-acoustic technique for measuring the enhancement. *Aerosol Sci Technol* 43:1006–1012.
19. Zhang R, et al. (2008) Variability in morphology, hygroscopicity, and optical properties of soot aerosols during atmospheric processing. *Proc Natl Acad Sci USA* 105:10291–10296.
20. Ghan SJ, Schwartz SE (2007) Aerosol properties and processes: A path from field and laboratory measurements to global climate models. *Bull Am Meteorol Soc* 88:1059–1083.
21. Hansen J, et al. (2007) Climate simulations for 1880–2003 with GISS modelE. *Clim Dynam* 29:661–696.
22. Clarke A, et al. (2007) Biomass burning and pollution aerosol over North America: Organic components and their influence on spectral optical properties and humidification response. *J Geophys Res* 112:D12S18.
23. Hoffer A, et al. (2006) Optical properties of humic-like substances (HULIS) in biomass-burning aerosols. *Atmos Chem Phys* 6:3563–3570.
24. Lewis K, Arnott WP, Moosmuller H, Wold CE (2008) Strong spectral variation of biomass smoke light absorption and single scattering albedo observed with a novel dual-wavelength photoacoustic instrument. *J Geophys Res* 113:D16203.
25. Jacobson MZ (1999) Isolating nitrated and aromatic aerosols and nitrated aromatic gases as sources of ultraviolet light absorption. *J Geophys Res* 104:3527–3542.
26. Sun H, Biedermann L, Bond TC (2007) Color of brown carbon: A model for ultraviolet and visible light absorption by organic carbon aerosol. *Geophys Res Lett* 34:L17813.
27. Roberts JM, et al. (2011) Isocyanic acid in the atmosphere and its possible link to smoke-related health effects. *Proc Natl Acad Sci USA* 108:8966–8971.
28. Cubison MJ, et al. (2011) Effects of aging on organic aerosol from open biomass burning smoke in aircraft and lab studies. *Atmos Chem Phys* 11:1680–7324.
29. Gyawali M, Arnott WP, Lewis K, Moosmuller H (2009) In situ aerosol optics inReno NV USA during and after the summer 2008 California wildfires and the influence of absorbing and non-absorbing organic coatings on spectral light absorption. *Atmos Chem Phys* 9:8007–8017.
30. Abel SJ, Haywood JM, Highwood EJ, Li J, Buseck PR (2003) Evolution of biomass burning aerosol properties from an agricultural fire in southern Africa. *Geophys Res Lett* 30:1783–1786.
31. Reid JS, et al. (2005) A review of biomass burning emissions part III: Intensive optical properties of biomass burning particles. *Atmos Chem Phys* 5:827–849.
32. Lack DA, Cappa CD (2010) Impact of brown and clear carbon on light absorption enhancement, single scatter albedo and absorption wavelength dependence of black carbon. *Atmos Chem Phys* 10:4207–4220.
33. Jacobson MZ (2012) Investigating cloud absorption effects: Global absorption properties of black carbon, tar balls, and soil dust in clouds and aerosols. *J Geophys Res* 117:D06205.
34. NOAA (2010) *Historical Meterological Data for Boulder, CO* (NOAA National Climatic Data Center), Available at www.ncdc.noaa.gov.
35. Alexander DTL, Crozier PA, Anderson JR (2008) Brown carbon spheres in east asian outflow and their optical properties. *Science* 321:833–836.
36. Posfai M, et al. (2004) Atmospheric tar balls: Particles from biomass and biofuel burning. *J Geophys Res* 109:D06213.
37. Kondo Y, et al. (2011) Emissions of black carbon, organic, and inorganic aerosols from biomass burning in North America and Asia in 2008. *J Geophys Res* 116:D08204.
38. Barnard JC, Volkamer R, Kassianov EI (2008) Estimation of the mass absorption cross section of the organic carbon component of aerosols in the Mexico City metropolitan area. *Atmos Chem Phys* 8:6665–6679.
39. Kirchstetter TW, Novakov T, Hobbs PV (2004) Evidence that the spectral dependence of light absorption by aerosols is affected by organic carbon. *J Geophys Res* 109:D21208.
40. Graham R, et al. (2011) *Fourmile Canyon Fire Preliminary Findings* (U.S. Department of Agriculture Forest Service, Rocky Mountain Research Station), Available at http://www.conservationgateway.org/sites/default/files/fourmile.pdf.
41. Langridge J, Richardson M, Law D, Lack DA, Murphy DM (2011) Aircraft instrument for comprehensive characterisation of aerosol optical properties, part I: Wavelength dependent optical extinction and its relative humidity dependence measured using cavity ringdown spectroscopy. *Aerosol Sci Technol* 45:1305–1318.
42. Lack D, et al. (2012) Aircraft instrumentation for comprehensive characterization of aerosol optical properties, Part 2: Black and brown carbon absorption and absorption enhancement measured with photo acoustic spectroscopy. *Aerosol Sci Technol* 46:555–568.
43. Thornberry T, et al. (2010) Persistence of organic carbon in heated aerosol residuals measured during tropical composition cloud and climate coupling (TC4). *J Geophys Res* 115:D00J02.
44. Lack DA, et al. (2008) Bias in filter based aerosol light absorption measurements due to organic aerosol loading: Evidence from ambient measurements. *Aerosol Sci Technol* 42:1033–1041.
45. Bahreini R, et al. (2009) Organic aerosol formation in urban and industrial plumes near Houston and Dallas, Texas. *J Geophys Res* 114:D00F16.
46. Allan JD, et al. (2003) Quantitative sampling using an Aerodyne aerosol mass spectrometer 1. Techniques of data interpretation and error analysis. *J Geophys Res* 108:4090–4099.
47. Bohren CF, Huffman DR (1983) *Absorption and Scattering of Light by Small Particles* (John Wiley & Sons, Inc., Hoboken, NJ) p 530.
48. Reid JS, Koppmann R, Eck TF, Eleuterio DP (2005) A review of biomass burning emissions part II: Intensive physical properties of biomass burning particles. *Atmos Chem Phys* 5:799–825.
49. Johnson BT, Osborne SR, Haywood JM, Harrison MAJ (2008) Aircraft measurements of biomass burning aerosol over West Africa during DABEX. *J Geophys Res* 113:D00C06.
50. Moosmuller H, Chakrabarty RK, Arnott WP (2009) Aerosol light absorption and its measurement: A review. *J Quant Spectrosc Radiat Transfer* 110:844–878.
51. Seinfeld JH, Pandis SN (1998) *Atmospheric Chemistry and Physics: From Air Pollution to Climate Change* (John Wiley and Sons, Inc., New York).
52. Bond TC, Bergstrom RW (2006) Light absorption by carbonaceous particles: An investigative review. *Aerosol Sci Technol* 40:27–67.
53. Mack LA, et al. (2010) Optical closure experiments for biomass smoke aerosols. *Atmos Chem Phys* 10:9017–9026.
54. Alfarra MR, et al. (2006) A mass spectrometric study of secondary organic aerosols formed from the photo- oxidation of anthropogenic and biogenic precursors in a reaction chamber. *Atmos Chem Phys* 6:5279–5293.
55. Adler G, Flores JM, Abo Riziq A, Borrmann S, Rudich Y (2011) Chemical, physical, and optical evolution of biomass burning aerosols: A case study. *Atmos Chem Phys* 11:1491–1503.
56. Weast RC (1985) *Hand Book of Chemistry and Physics* (CRC Press, Boca Raton, Fl).